

## Condensed-Phase Relaxation of Multilevel Quantum Systems. II. Comparison of Path Integral Calculations and Second-Order Relaxation Theory for a Nondegenerate Three-Level System<sup>†</sup>

Simone Peter,<sup>‡</sup> Deborah G. Evans,<sup>\*,§</sup> and Rob D. Coalson<sup>‡</sup>

Department of Chemistry, University of Pittsburgh, Pittsburgh, Pennsylvania 15260, and

Department of Chemistry, University of New Mexico, Albuquerque, New Mexico 87131

Received: February 24, 2006; In Final Form: May 13, 2006

An exactly solvable model of multisite condensed-phase vibrational relaxation was studied in Paper I (Peter, S.; Evans, D. G.; Coalson, R. D. *J. Phys. Chem. B* 2006, 110, 18758.), where it was shown that long-time steady-state site populations of a degenerate  $N$ -level system are not equal (hence, they are non-Boltzmann) and depend on the initial preparation of the system and the number of sites that it comprises. Here we consider a generalization of the model to the case of a nondegenerate three-level system coupled to a high-dimensional bath: such a model system has direct relevance to a large class of donor–bridge–acceptor electron transfer processes. Because the quantum dynamics of this system cannot be computed analytically, we compare numerically exact path integral calculations to the predictions of second-order time-local relaxation theory. For modest system–bath coupling strengths, the two sets of results are in excellent agreement. They show that non-Boltzmann long-time steady-state site populations are obtained when the level splitting is small but nonzero, whereas at larger values of the system bias (asymmetry) these populations become Boltzmann distributed.

### 1. Introduction

An exactly solvable model of multilevel condensed-phase vibrational relaxation was studied in a companion paper (hereafter referred to as Paper I<sup>1</sup>). In this model, a set of  $N$  degenerate states (e.g., sites on a lattice) couple to each other via nearest-neighbor hopping matrix elements and to a high dimensional harmonic oscillator bath via a particular type of system–bath coupling. It was shown in Paper I that the long-time steady-state site populations are not equal (for  $N > 2$ ) and thus are not distributed according to the Boltzmann formula familiar from equilibrium statistical mechanics. (Precise details depend on the initial conditions under which the system as prepared as well as the value of  $N$ .) This model represents a subset of system–bath Hamiltonians for which exact quantum dynamics can be computed using the general formulation developed in ref 2. The advantage of such exactly solvable system–bath problems lie in the fact that they can be used as “benchmarks” to test the wide variety of approximate methods that have been devised to study the time-evolution of dissipative quantum systems.<sup>3–28</sup>

In the present paper, the form of the model Hamiltonians in Paper I is generalized to the case of a nondegenerate  $N$ -level system coupled to a dissipative bath. This study clearly increases the applicability of the models to more general experimentally relevant problems. For example, it enables us to study of the dynamics of model Hamiltonians that can be directly mapped onto the class of processes involving electron transfer from a donor state to an acceptor state through a bridge (or D–B–A systems),<sup>29–32</sup> exciton dynamics in light-harvesting com-

plexes,<sup>33–38</sup> and vibrational energy relaxation in the condensed phase.<sup>11,39,40</sup>

Several somewhat surprising conclusions were gleaned for the degenerate limit system analyzed in Paper I;<sup>1</sup> in particular, the origin of the unequal long-time populations observed in the  $N$ -level system are not immediately obvious. In fact, application of the Pauli master equations (first-order rate equations for the site probabilities, with each pair of sites coupled by appropriate forward and backward rate constants<sup>41</sup>) to the system–bath Hamiltonians of the type studied would result in equal populations of each of the degenerate localized states after equilibration.

Because the Pauli master equations emerge directly as a consequence of second-order relaxation theory (vide infra), we would not expect them to apply in the case of strong system–bath coupling. However, the unequal distribution of steady-state populations illustrated for the general  $N$ -level system in Paper I are completely independent of bath characteristics, and thus they certainly hold when the system–bath coupling is weak. As noted above, they are not consistent with the prediction of the Pauli master equations. Perhaps second-order relaxation theory itself breaks down? In fact, we know<sup>2</sup> that second-order local relaxation theory (RT) is exact for this class of Hamiltonians, so there must be a problem with the reduction of second-order RT to Pauli master equations (PMEs) for these systems. Indeed, derivation of the PME from second-order RT requires an important additional approximation, namely, a rotating wave approximation (or RWA,<sup>41</sup> in which rapidly oscillating terms on the rhs of the full second-order RT differential equations are neglected). In magnetic resonance theory, second-order RT is known as Redfield theory. The rapidly oscillating terms just alluded to are termed “nonsecular”, and neglect of these constitutes the secular approximation to the Redfield equations.<sup>42</sup>

<sup>†</sup> Part of the special issue “Robert J. Silbey Festschrift”.

<sup>\*</sup> Corresponding author. E-mail: debi@unm.edu.

<sup>‡</sup> University of Pittsburgh.

<sup>§</sup> University of New Mexico.

The validity of this approximation requires that if  $\tau$  is the time over which the system reduced density matrix evolves by a significant amount, then  $(E_j - E_k)\tau \gg 1$  for any pair of zeroth-order energy levels. The value of  $\tau$  is controlled by the strength of the system–bath coupling: smaller system–bath coupling corresponds to larger  $\tau$ . Thus, if our  $N$ -level system is nondegenerate (no two zeroth-order energy levels are the same), then for sufficiently small system–bath coupling the PME's should become valid and the asymptotic values of the site populations should be given by the Boltzmann distribution [i.e., relative probability of state  $j$  given by  $\exp(-\beta E_j)$ , with  $\beta = 1/kT$ ,  $k$  being Boltzmann's constant and  $T$  the absolute temperature].

However, for a completely symmetric  $N$ -level system of the type studied in Paper I, the conditions of validity of the RWA are not satisfied for any finite system–bath coupling strength, no matter how weak. We must appeal to the full second-order RT equations of motion, and evidently (because they are exact for the symmetric dissipative  $N$ -level systems considered in Paper I) these predict dynamics and long-time steady states considerably different from the results obtained via the PME's.

This raises another interesting question. If the asymmetry of an  $N$ -level system is increased gradually from none (completely symmetric  $N$ -level system) to a situation where all zeroth-order energy levels are well separated in energy, will the steady-state site populations morph between “non-Boltzmann” values for small asymmetry and “Boltzmann” values for larger asymmetry? To obtain a reliable answer to this question, we need a way to compute the exact quantum dynamics for an asymmetric  $N$ -level system coupled to a harmonic oscillator bath in the manner being considered here. The analytical solution presented in Paper I does not apply in this case. However, the tensor product path integral (PI) technique<sup>43–45</sup> can be used to generate numerically exact results, albeit at considerable computational effort. We can then compare the numerical PI results to numerical results via second-order local RT (obtained with much less computational effort).

The outline of the present paper is as follows: In Section 2, the model system–bath Hamiltonian is introduced, and its general method of solution via the tensor product path integral (PI) algorithm and second-order relaxation theory is reviewed. In Section 3, we explore the dynamics of a three-level quantum system coupled off-diagonally to a condensed phase environment. The evolution of the reduced density matrix elements of the system is calculated using both the transfer matrix PI algorithm and a second-order perturbative solution of the Liouville equation for the system–bath Hamiltonian. Excellent agreement between the two methods is found. Finally, Section 4 contains a discussion of our principal findings.

## 2. Model Hamiltonian and Reduced System Dynamics

Our goal is to study nondegenerate  $N$ -level systems characterized by nearest-neighbor off-diagonal coupling to a dissipative bath. For concreteness and computational tractability, we focus our attention in what follows primarily on the case that  $N = 3$ . To precisely state the problem of interest, we presume that the three-level system Hamiltonian  $\hat{H}_s$  has the form

$$\hat{H}_s = \epsilon \begin{bmatrix} 1 & 0 & 0 \\ 0 & 0 & 0 \\ 0 & 0 & -1 \end{bmatrix} \quad (1)$$

where  $\epsilon$  is a real parameter with energy units. In an electron-transfer process involving hopping between three localized electronic states (donor, bridge, and acceptor), the on-diagonal

elements of this matrix correspond to diagonal matrix elements of an effective one-electron electronic Hamiltonian in the basis of these site-localized states.

We seek to compute the quantum dynamics of such a three-site system coupled to a condensed phase environment. The total system–bath Hamiltonian ( $\hat{H}$ ) can be written as

$$\hat{H} = \hat{H}_s + \hat{R}_s \hat{R}_b + \hat{H}_b \quad (2)$$

where  $\hat{H}_b$  is the isolated bath Hamiltonian, and  $\hat{R}_b$  is the bath operator involved in the system–bath coupling term. We will choose  $\hat{H}_b$  here to be a collection of uncoupled unit mass harmonic oscillators and  $\hat{R}_b$  to be a linear combination of bath coordinates: that is,  $\hat{H}_b = (1/2)\sum_j(\hat{p}_j^2 + \omega_j^2\hat{q}_j^2)$  and  $\hat{R}_b = \sum_j c_j \hat{q}_j$ , where each oscillator (with frequency  $\omega_j$ ) is coupled to the system coordinate via  $c_j$ . The values of the coupling constants,  $c_j$ , are conveniently encoded in the spectral density function

$$J(\omega) = \frac{\pi}{2} \sum_j \frac{c_j^2}{\omega_j} \delta(\omega - \omega_j) \quad (3)$$

The system operator  $\hat{R}_s$  in the system–bath coupling term consists, as noted above, of nearest-neighbor hopping matrix elements:

$$\hat{R}_s = \begin{pmatrix} 0 & 1 & 0 \\ 1 & 0 & 1 \\ 0 & 1 & 0 \end{pmatrix} \quad (4)$$

Thus, the physical effect of the system–bath coupling under consideration is to add fluctuations to the hopping matrix elements. The details of the fluctuations depend on the details of  $\hat{H}_b$  and  $\hat{R}_b$ , and the role of the bath in the reduced system density matrix is entirely captured by the bath correlation function  $\langle \hat{R}_b(t) \hat{R}_b \rangle$ .<sup>42</sup>

We will consider initial density operators of the form  $\hat{\Gamma}(0) = \hat{\rho}_\beta \otimes \hat{\rho}(0)$ , where  $\hat{\Gamma}(t)$  is the complete system–bath density matrix at time  $t$ , and  $\hat{\rho}(0)$  is the initial system density operator;  $\hat{\rho}_\beta$  is the thermal density matrix for the bath at inverse temperature  $\beta$ , that is,  $\hat{\rho}_\beta = \exp(-\beta \hat{H}_b)/Z_b$  with  $Z_b = \text{tr}_b\{\exp(-\beta \hat{H}_b)\}$ , where  $\text{tr}_b$  indicates trace over all bath degrees of freedom. We wish to extract elements of the reduced system density matrix in the site basis:  $\hat{\rho}_{JK}(t) = \text{tr}_b\{\langle J|\hat{\Gamma}(t)|K\rangle\}$ .

The Hamiltonian in eq 2 is thus a generalization for  $N = 3$  of the Hamiltonian studied in Paper I (cf. eq 2 of that paper, with  $\alpha = 0$ )<sup>1</sup> to the case of a nondegenerate system Hamiltonian parametrized by  $\epsilon \neq 0$ . Unfortunately, when  $\epsilon \neq 0$  it is no longer true that  $[\hat{H}_s, \hat{R}_s] = 0$ , and the system–bath Hamiltonian in eq 2 does not admit exact closed-form solutions of the type discussed in Paper I.<sup>1,2</sup> Nevertheless, the degenerate systems studied in Paper 1 (corresponding to  $\epsilon = 0$  in eq 1) provide a suitable point of departure for analyzing the effects of increasing the splitting of the levels in the three-level system.

As shown in Paper 1,<sup>1</sup> when a *degenerate*  $N$ -level system initially localized on the  $l$ th state is coupled to a bath according to eq 2 and with the bath autocorrelation function written as  $\langle \hat{R}_b(t) \hat{R}_b(0) \rangle = \kappa(t) - i\xi(t)$ , the reduced system density matrix dynamics can be written exactly and explicitly as

$$\rho_{LM}(t) = \left( \frac{2}{N+1} \right)^2 \sum_{j=1}^N \sum_{r=1}^N A_{j,r}(t) \sin(Lj\theta) \sin(Mr\theta) \sin(Ij\theta) \sin(Ir\theta) \quad (5)$$

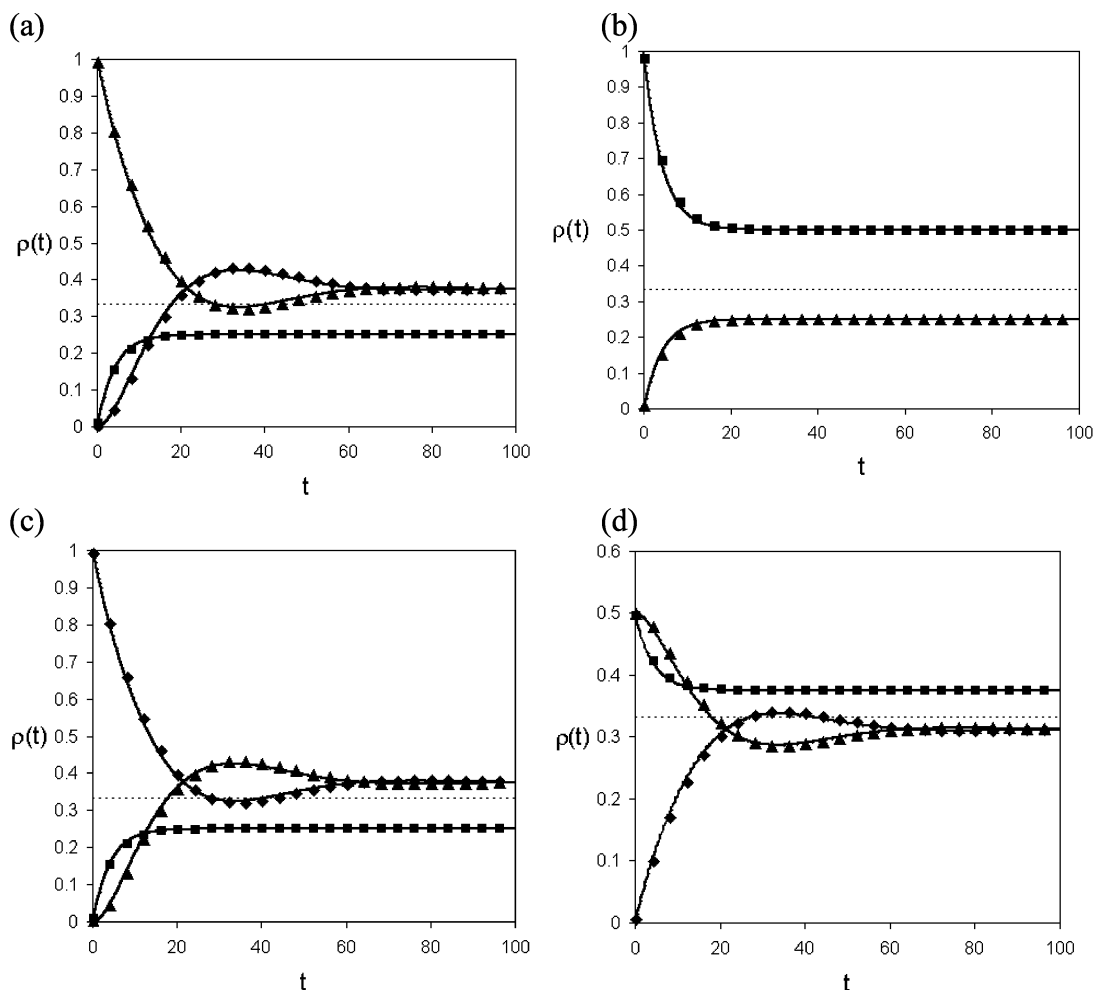


**Figure 1.** Evolution of the reduced system density matrix elements: (i)  $\rho_{11}(t)$  (triangles), (ii)  $\rho_{22}(t)$  (squares), and (iii)  $\rho_{33}(t)$  (diamonds) of a degenerate three-level system in an Ohmic bath ( $\eta = 0.01$ ,  $\omega_c = 7.5$ ,  $\beta = 0.5$ ) with different system density matrix initial conditions: (a)  $\rho_{11}(0) = 1$ , (b)  $\rho_{22}(0) = 1$ , (c)  $\rho_{33}(0) = 1$ , (d)  $\rho_{11}(0) = \rho_{22}(0) = 1/2$  (all other density matrix elements being 0). Path integral calculations (points) are compared to the exact solutions from Paper I (solid lines)<sup>1</sup> and second-order RT (solid lines, superimposed). The dotted line indicates the expected Boltzmann population of each level of the three-level system at equilibrium.

where

$$A_{j,r}(t) \equiv \exp\left[\int_0^t \int_0^{t'} dt' dt'' [-\kappa(t' - t'')(\lambda_j - \lambda_r)^2 + i\xi(t' - t'')(\lambda_j^2 - \lambda_r^2)]\right]$$

is given in terms of the eigenvalues  $\lambda_j$  of  $\hat{R}_s$ .

For *nondegenerate* ( $\epsilon \neq 0$ )  $N$ -level systems coupled via the analogue of eq 2, other methods must be used to generate solutions of the reduced system dynamics. A tensor product path integral approach gives numerically exact solutions of the reduced system dynamics in the weak system–bath coupling regime.<sup>43–45</sup> Approximate reduced system density matrix dynamics can also be predicted using standard second-order time-local relaxation theory.

Approximate second-order equations of motion for the reduced system density matrix evolving under the system–bath Hamiltonian in eq 2 can be obtained in the interaction picture using  $\hat{H}_0 = \hat{H}_s + \hat{H}_b$  as the zeroth-order Hamiltonian. The local equations of motion of the reduced system density matrix in the interaction picture,  $\hat{\rho}_I(t)$ , to second order in the system–bath coupling, take the form<sup>46,47</sup>

$$\dot{\hat{\rho}}_I(t) = - \int_0^t dt' \{ \langle \hat{R}_b(t) \hat{R}_b(t') \rangle [\hat{R}_s(t), \hat{R}_s(t') \hat{\rho}_{SI}(t')] - \langle \hat{R}_b(t) \hat{R}_b(t') \rangle [\hat{R}_s(t), \hat{\rho}_{SI}(t) \hat{R}_s(t')] \} \quad (6)$$

Second-order time-local relaxation theory has been shown to be exact for systems where  $[\hat{H}_s, \hat{R}_s] = 0$ .<sup>2</sup> Thus, for degenerate  $N$ -level systems (when  $\epsilon = 0$ ), the standard second-order local RT should give the same results as the exact solution given by eq 5.

In the general case, using  $\hat{H}_s$  in eq 1, it is expected that second-order relaxation equations will give reasonably accurate solutions in the limit where the system–bath coupling term is small. In general, eq 6 is most conveniently solved as a set of coupled first-order ordinary differential equations by writing the  $N \times N$  reduced system density matrix as an  $N^2$ -dimensional vector, and carrying out the numerical integration with a simple Runge–Kutta algorithm.

Using the tensor product path integral algorithm, it is possible to generate numerically exact solutions of the evolution of the reduced system density matrix for general Hamiltonians given in eq 2 when  $\epsilon \neq 0$ . This will allow us to compare these numerical answers directly with those obtained using the approximate local second-order relaxation theory equations of motion.

The tensor product path integral algorithm has been developed for system–bath problems of the form<sup>43</sup>

$$\hat{H} = \hat{H}_s + \hat{H}_b + \sum_j \frac{1}{2} \omega_j^2 \left( \hat{q}_j - \frac{c_j}{\omega_j^2} \hat{S} \right)^2 \quad (7)$$

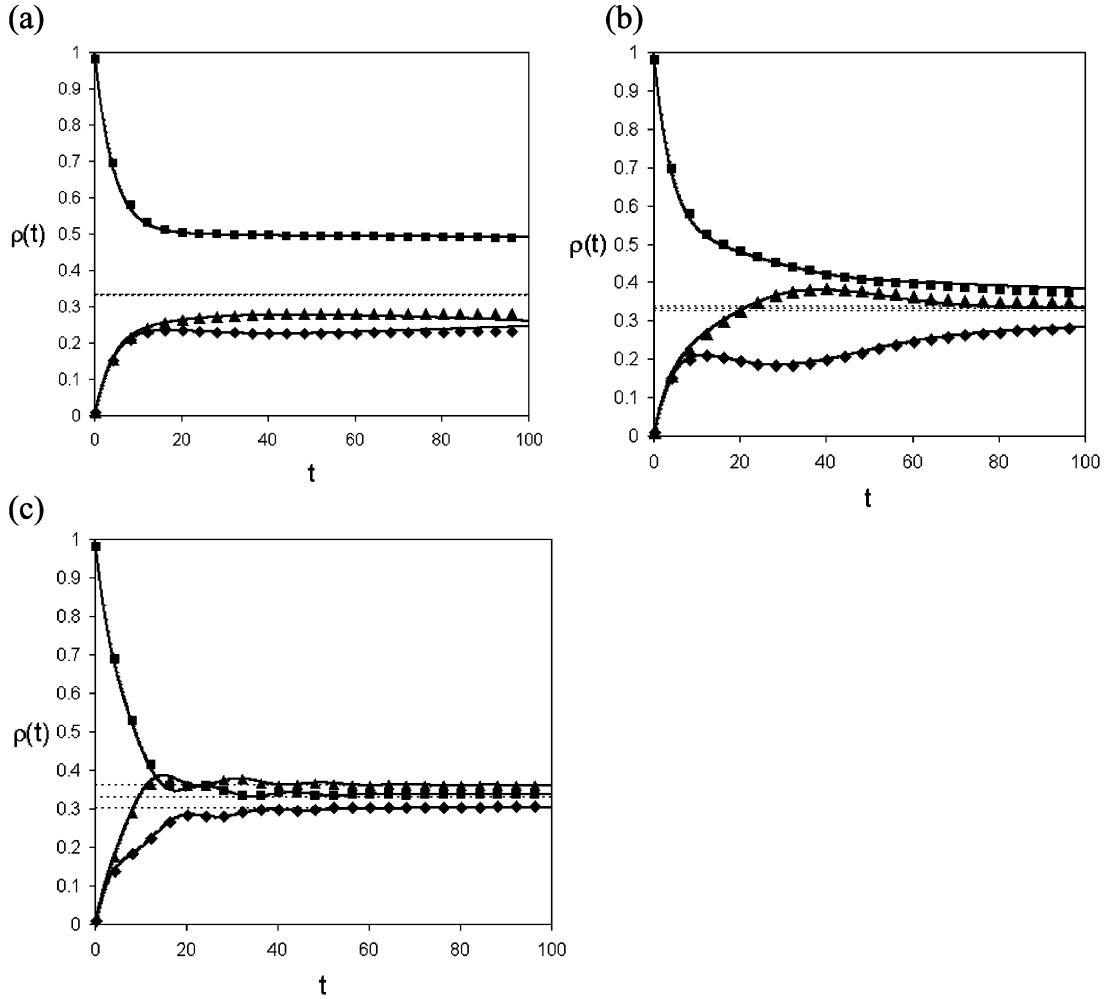


**Figure 2.** Evolution of the reduced system density matrix elements:  $\rho_{11}(t)$  (triangles),  $\rho_{22}(t)$  (squares), and  $\rho_{33}(t)$  (diamonds) of a three-level system coupled to an Ohmic bath ( $\eta = 0.01$ ,  $\omega_c = 7.5$ ,  $\beta = 0.5$ ), for different values of the system bias: (a)  $\epsilon = 0.006$ , (b)  $\epsilon = 0.03$ , and (c)  $\epsilon = 0.18$ ; the initial system density matrix is taken as  $\rho_{22}(0) = 1$  (all other density matrix elements being 0). Path integral calculations (discrete points) are compared with local second-order relaxation theory (solid lines). Dotted lines indicate the expected Boltzmann population of the system states at equilibrium.

where  $\hat{S}$  is a diagonal system operator. The Hamiltonian as written above does not transparently correspond to the generic Hamiltonians in eq 2 because  $\hat{R}_s$  is not diagonal in the system coordinate space. The Hamiltonian in eq 2 needs to be transformed in order to apply the tensor product path integral algorithm to this problem. This is achieved for the case that  $N = 3$  using the unitary matrix,  $\hat{T}$

$$\hat{T} = \frac{1}{\sqrt{2}} \begin{bmatrix} (1/\sqrt{2}) & -1 & (1/\sqrt{2}) \\ -1 & 0 & 1 \\ (1/\sqrt{2}) & 1 & (1/\sqrt{2}) \end{bmatrix}$$

that diagonalizes  $\hat{R}_s$  and transforms the system operators  $\hat{H}_s$  and  $\hat{\rho}$  in eq 2. In particular, the initial system density matrix is transformed as  $\hat{\rho}'(0) = \hat{T}^{-1}\hat{\rho}(0)\hat{T}$ ,  $\hat{S} = -\hat{T}^{-1}\hat{R}_s\hat{T}$  and  $\hat{H}_s' = \hat{T}^{-1}\hat{H}_s\hat{T} - \hat{S}^2\sum_j(c_j^2/2\omega_j^2)$ . The implementation of the transfer matrix path integral algorithm is accomplished by calculating the system propagator in terms of the eigenvectors and eigenvalues of the matrix  $\hat{H}_s'$ . The evolving reduced system density matrix must then be back-transformed at each step of the tensor-product propagation to obtain the reduced system density matrix in the original representation.

There are two sources of numerical error using the transfer matrix path integral algorithm. Application of the Trotter product formula to the propagator is in principle exact only if  $\hat{H}_s'$  and

$\hat{S}$  commute. Although this is the case for degenerate  $N$ -level systems, for nondegenerate systems the error is expected to grow as the path integral time slice increases. In addition, the application of the tensor product algorithm requires successive approximations to the bath response function in the influence functional. Convergence of the path integral is obtained by increasing the extent of the short-range temporal nonlocality of the influence functional. In this way, increased accuracy of the path integral method is achieved, but at the expense of increasingly large demands on computer time and memory. In practice, convergence can be attained only for relatively weak system–bath coupling and modest values of the system energy level bias,  $\epsilon$ .

### 3. Quantum Dynamics of Dissipative Three-Level Systems

It is easy to verify from the exact solution presented in eq 15 of Paper I<sup>1</sup> that for a degenerate three-level system coupled to a dense collection of bath modes and an initial system density matrix given by  $\rho_{JK}(0) = \delta_{J,2}\delta_{K,2}$  (and thus  $\rho_{22}(0) = 1$ ,  $\rho_{11}(0) = \rho_{33}(0) = 0$ ), then  $(\rho_{11}(\infty), \rho_{22}(\infty), \rho_{33}(\infty)) = (1/4, 1/2, 1/4)$ . In contrast, when  $\rho_{JK}(0) = \delta_{J,1}\delta_{K,1}$  (and thus  $\rho_{11}(0) = 1$ ,  $\rho_{22}(0) = \rho_{33}(0) = 0$ ), then  $(\rho_{11}(\infty), \rho_{22}(\infty), \rho_{33}(\infty)) = (3/8, 1/4, 3/8)$ .

This behavior may seem odd, in that we have a system in which all site energies are the same (namely, zero), so that naïve application of the Boltzmann distribution formula would imply



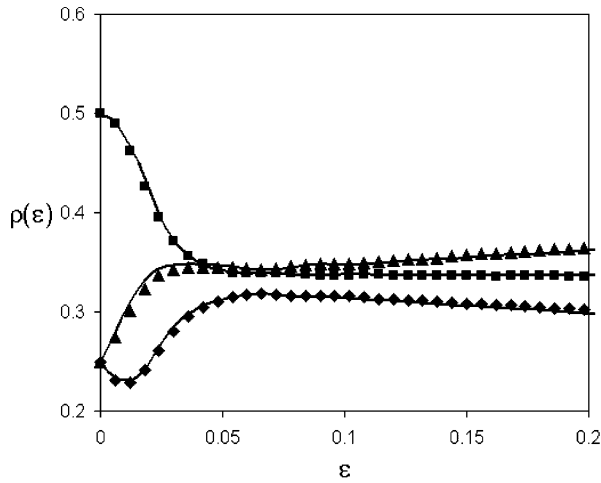


**Figure 3.** Long-time limits (at  $t = 100$ ) of the reduced density matrix elements:  $\rho_{11}$  (triangles),  $\rho_{22}$  (squares), and  $\rho_{33}$  (diamonds) of a three-level system coupled to an Ohmic bath ( $\eta = 0.01$ ,  $\omega_c = 7.5$ ,  $\beta = 0.5$ ) as a function of  $\epsilon$ , the system bias. Path integral calculations (discrete points) are compared directly with the prediction of local second-order relaxation theory (solid lines) using the initial condition,  $\rho_{22}(0) = 1$  (all other density matrix elements being 0).

that if the long-time steady state represents Boltzmann equilibrium at temperature  $T$ , then all three states should be equally populated, independent of their initial populations. Indeed, application of the Pauli master equations to a system–bath coupling problem of the present type implies precisely this equal population property.

**3.1. Reduced System Dynamics of a Degenerate Three-Level System.** The first step in our study is to use the analytical expressions for degenerate three-level systems discussed in Paper I<sup>1</sup> to check the performance of the path integral algorithm and second-order relaxation theory for the bath parameters used in subsequent studies. To this end, we have chosen a specific spectral density for the bath, namely, an Ohmic spectral density  $J(\omega) = \eta\omega e^{-\omega/\omega_c}$ , defined in terms of a coupling strength to the bath,  $\eta$ , and a cutoff frequency,  $\omega_c$ . The path integral computer code and the analytical expressions in eq 5<sup>1</sup> should, to within numerical convergence and round-off errors, give the same result for degenerate systems. Although agreement between all three methods is expected to be good in this case, it will provide confirmation that the path integral code has

achieved convergence for the particular numerical parameters chosen, and that the second-order perturbation theory is being implemented accurately.

In Figure 1, the diagonal reduced system density matrix elements are plotted as a function of time. The results using the exact solutions from eq 5 are compared with the path integral algorithm and local second-order relaxation theory. The evolution of the system density matrix is plotted for different initial conditions (specifically, nonzero initial system density matrix elements): (a)  $\rho_{11}(0) = 1$ , (b)  $\rho_{22}(0) = 1$ , (c)  $\rho_{33}(0) = 1$ , and (d)  $\rho_{11}(0) = \rho_{22}(0) = 1/2$ , and an Ohmic bath characterized by  $\eta = 0.01$ ,  $\omega_c = 7.5$  and inverse temperature  $\beta = 0.5$ .

The agreement between all three methods is seen to be very good, irrespective of the particular initial system state chosen. The long-time asymptotic limits are captured accurately by both the path integral calculations and the second-order perturbation theory. This provides confidence in the accuracy of the results obtained via these algorithms for *biased* system calculations (presented in the following subsection), where no analytical formulas are available for comparison.

**3.2. Reduced Dynamics for Dissipative Nondegenerate (Biased) Systems.** We have used the tensor product path integral algorithm to study nondegenerate three-level systems coupled to a dissipative Ohmic bath using  $\hat{H}_s$  given in eq 1. Of particular interest is the long-time behavior of these three-level systems and, especially, how the long-time limit of the system site populations may differ from the corresponding populations predicted by standard second-order relaxation theory for condensed-phase systems.

In Figure 2, a comparison of the results using the numerically exact path integral calculations and the second-order local equations of motion is shown for increasing values of  $\epsilon$ , with the initial system density matrix  $\rho_{22}(0) = 1$  (all other elements being 0). An Ohmic bath with  $\eta = 0.01$ ,  $\omega_c = 7.5$  and inverse temperature  $\beta = 0.5$  is coupled to the system with (a)  $\epsilon = 0.006$ , (b)  $\epsilon = 0.03$ , and (c)  $\epsilon = 0.18$ .

The parameters chosen for the Ohmic bath are the same as the bath considered in Figure 1. As the bias between the three levels is increased, the local second-order equations are expected to remain accurate because the second-order perturbation approximation to the quantum Liouville equation is made in terms of the strength of the system–bath coupling (*vide supra*). The numerically exact path integral calculations show good

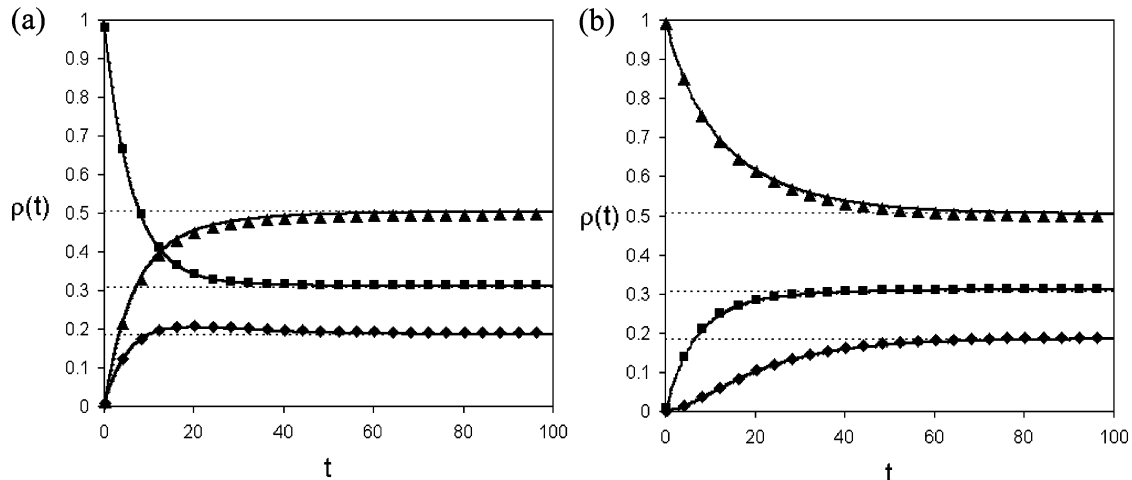


**Figure 4.** Evolution of the reduced density matrix elements of a biased three-level system,  $\epsilon = 1.0$ , coupled to an Ohmic bath ( $\eta = 0.01$ ,  $\omega_c = 7.5$ ,  $\beta = 0.5$ ).  $\rho_{11}(t)$  (triangles),  $\rho_{22}(t)$  (squares), and  $\rho_{33}(t)$  (diamonds) are shown for the initial system density matrix given by (a)  $\rho_{22}(0) = 1$  and (b)  $\rho_{11}(0) = 1$  (all other density matrix elements being 0). Path integral calculations (discrete points) are shown in comparison to local second-order relaxation theory (solid lines). Dotted lines indicate the expected Boltzmann population of the system levels at equilibrium.

agreement with the results from the second-order relaxation theory as regards both the long-time non-Boltzmann limits and the temporal relaxation dynamics. In Figure 2, it is interesting that at small values of the bias the long-time limit of the reduced system density matrix elements deviate significantly from the Boltzmann populations predicted by the Pauli master equations. As the bias in the system Hamiltonian is increased, these long-time populations converge to their Boltzmann-distribution values.

In Figure 3, the long-time limits (taken after  $t = 100$ ) for the exact path integral calculations and the second-order relaxation theory are plotted as a function of the system bias,  $\epsilon$ . As can be seen from Figure 3, as the value of  $\epsilon$  is increased from zero, the site occupation probabilities go from being significantly non-Boltzmann (at small  $\epsilon$ ) to completely in agreement with the Boltzmann distribution (at larger  $\epsilon$ ). It is also important to note that the agreement between the path integral calculations and the second-order relaxation theory is excellent over the entire range of  $\epsilon$  values considered.

In Figure 4, results for the time evolution of the reduced system density matrix are shown when the system bias is relatively large, namely,  $\epsilon = 1.0$ . In panel (a)  $\rho_{22}(0) = 1$ , and in panel (b)  $\rho_{11}(0) = 1$  (all other elements of the initial system density matrix being 0 in each case). The long-time populations for large bias and high temperature approach the Boltzmann distribution limit. At larger values of the system bias, the asymptotic occupation probabilities are clearly independent of where the system density is initially localized.

The results presented in Figures 2–4 indicate that second-order local RT (eq 6) performs remarkably well for this general system–bath coupling problem, provided that the system–bath coupling is relatively weak. The small differences between the PI and RT data that are seen in Figures 2 and 3 are within the error bars associated with the numerical convergence of the path integral calculations. Second-order local RT is capable of describing the entire regime of quantum dynamics ranging from the completely symmetric three-level system (with long-time site populations that are non-Boltzmann and depend on initial system preparation) to a “strongly” asymmetric three-level system (with Boltzmann distributed long-time site populations that are independent of initial system preparation). This behavioral transition is intimately connected with the onset of reliability of the RWA as system bias increases.

#### 4. Discussion

In this paper, we have extended our study of degenerate  $N$ -level quantum systems coupled to a dissipative bath that were solved analytically in Paper I<sup>1</sup> to the case of nondegenerate  $N$ -level systems. In particular, we have used a number of methods to study the dynamics of a three-level system ( $N = 3$ ) with energetically inequivalent sites that are coupled off-diagonally to an environment of harmonic bath coordinates characterized by a continuous spectral density.

The quantum dynamics problem of a nondegenerate  $N$ -level system coupled to a bath as considered herein does not admit an exact analytical solution. Thus, we have used numerically exact path integral calculations and second-order relaxation theory to study the relaxation dynamics of a nondegenerate three-level system coupled to an Ohmic bath. These two methods show surprisingly good agreement when the system–bath coupling strength is modest, and both methods show that a non-Boltzmann limit in the reduced system density matrix is attainable when the level splitting between the localized states is sufficiently small, consistent with the  $\epsilon \rightarrow 0$  limit analyzed

in Paper I. We have also been able to demonstrate that at larger values of the system bias the reduced density matrix elements tend to those predicted by the Boltzmann formula (based on the values of the diagonal elements of  $\hat{H}_s$ ).

Future work will use these methodologies to study experimental problems that can be represented by the model introduced in this paper. In particular, the success of second-order local relaxation theory over the entire parameter space considered in the present study bodes well for its application in more complex systems (e.g., characterized by  $N > 3$ ), where the tensor product PI algorithm will be difficult to implement.

**Acknowledgment.** D.G.E. is a Cottrell Scholar of the Research Corporation and a Camille Dreyfus Teacher-Scholar. D.G.E.’s work is partially supported by a grant from the Petroleum Research Fund (PRF no. 43207-AC10) administered by the ACS. R.D.C.’s work was partially supported by a grant from the National Science Foundation.

#### References and Notes

- (1) Peter, S.; Evans, D. G.; Coalson, R. D. *J. Phys. Chem.* **2006**, *110*, 18758.
- (2) Coalson, R. D.; Evans, D. G. *Chem. Phys.* **2004**, *296*, 117.
- (3) Harris, R. A.; Silbey, R. J. *Chem. Phys.* **1983**, *78*, 7330.
- (4) Parris, P. E.; Silbey, R. J. *Chem. Phys.* **1985**, *83*, 5619.
- (5) Rackovsky, S.; Silbey, R. *Mol. Phys.* **1973**, *25*, 61.
- (6) Reichman, D. R.; Silbey, R. J. *J. Chem. Phys.* **1996**, *104*, 1506.
- (7) Silbey, R. *Annu. Rev. Phys. Chem.* **1976**, *27*, 203.
- (8) Silbey, R.; Harris, R. A. *J. Chem. Phys.* **1984**, *80*, 2615.
- (9) Silbey, R.; Harris, R. A. *J. Phys. Chem.* **1989**, *93*, 7062–7071.
- (10) Jang, S.; Cao, J. S.; Silbey, R. J. *J. Chem. Phys.* **2002**, *116*, 2705–2717.
- (11) Suarez, A.; Silbey, R.; Oppenheim, I. *J. Chem. Phys.* **1992**, *97*, 5101–5107.
- (12) Jang, S.; Newton, M. D. *J. Chem. Phys.* **2005**, *122*, 024501.
- (13) Kubo, R.; Toyozawa, Y. *Prog. Theor. Phys.* **1955**, *13*, 160–182.
- (14) Redfield, A. *Adv. Magn. Reson.* **1965**, *1*, 1.
- (15) Jean, J. M.; Friesner, R. A.; Fleming, G. R. *J. Chem. Phys.* **1992**, *96*, 5827–5842.
- (16) Pollard, W. T.; Felts, A. K.; Friesner, R. A. *Adv. Chem. Phys.*, Vol. **XCIII** **1996**, *93*, 77–134.
- (17) Walsh, A. M.; Coalson, R. D. *Chem. Phys. Lett.* **1992**, *198*, 293–299.
- (18) Gaspard, P.; Nagaoka, M. *J. Chem. Phys.* **1999**, *111*, 5668–5675.
- (19) Sparpaglione, M.; Mukamel, S. *J. Chem. Phys.* **1988**, *88*, 3263–3280.
- (20) Golosov, A. A.; Friesner, R. A.; Pechukas, P. J. *J. Chem. Phys.* **1999**, *110*, 138–146.
- (21) Laird, B. B.; Budimir, J.; Skinner, J. L. *J. Chem. Phys.* **1991**, *94*, 4391–4404.
- (22) Davies, E. B. *Commun. Math. Phys.* **1974**, *39*, 91–110.
- (23) Dumcke, R.; Spohn, H. *Z. Phys. B: Condens. Matter* **1979**, *34*, 419–422.
- (24) Egorova, D.; Kuhl, A.; Domcke, W. *Chem. Phys.* **2001**, *268*, 105–120.
- (25) Zwanzig, R. *Physica* **1964**, *30*, 1109.
- (26) Kohen, D.; Marston, C. C.; Tannor, D. J. *J. Chem. Phys.* **1997**, *107*, 5236–5253.
- (27) Wilkie, J. J. *J. Chem. Phys.* **2001**, *114*, 7736–7745.
- (28) Yan, Y. J.; Shuang, F.; Xu, R. X.; Cheng, J. X.; Li, X. Q.; Yang, C.; Zhang, H. Y. *J. Chem. Phys.* **2000**, *113*, 2068–2078.
- (29) Hayes, R.; Wasielewski, M.; Gosztola, D. *J. Am. Chem. Soc.* **2000**, *122*, 5563.
- (30) Davis, W.; Ratner, M.; Wasielewski, M. *J. Am. Chem. Soc.* **2001**, *123*, 7877.
- (31) Scherer, T.; Vanstokkum, I.; Brouwer, A.; Verhoeven, J. *J. Phys. Chem.* **1994**, *98*, 10539.
- (32) Skourtis, S.; Archontis, G.; Xie, Q. J. *J. Chem. Phys.* **2001**, *115*, 9444.
- (33) Jean, J. M. *J. Chem. Phys.* **1994**, *101*, 10464–10473.
- (34) Jean, J. M.; Fleming, G. R. *J. Chem. Phys.* **1995**, *103*, 2092–2101.
- (35) Jean, J. M. *J. Phys. Chem. A* **1998**, *102*, 7549–7557.
- (36) Cina, J. A.; Fleming, G. R. *J. Phys. Chem. A* **2004**, *108*, 11196–11208.
- (37) Yang, M.; Fleming, G. R. *Chem. Phys.* **2002**, *282*, 161.
- (38) Jang, S.; Jung, Y. J.; Silbey, R. J. *J. Chem. Phys.* **2002**, *275*, 319–332.
- (39) Figueirido, F. E.; Levy, R. M. *J. Chem. Phys.* **1992**, *97*, 703–706.

- (40) Oxtoby, D. W. *Annu. Rev. Phys. Chem.* **1981**, 32, 77–101.
- (41) Blum, K. *Density Matrix Theory and Applications*, 2nd ed.; Plenum Press: New York, 1996.
- (42) Schatz, G. C.; Ratner, M. A. *Quantum Mechanics in Chemistry*; Dover Publications: Mineola, NY, 2002.
- (43) Makarov, D. E.; Makri, N. *Chem. Phys. Lett.* **1994**, 221, 482–491.
- (44) Makri, N.; Makarov, D. E. *J. Chem. Phys.* **1995**, 102, 4600–4610.
- (45) Makri, N.; Makarov, D. E. *J. Chem. Phys.* **1995**, 102, 4611–4618.
- (46) Mukamel, S.; Oppenheim, I.; Ross, J. *Phys. Rev. A* **1978**, 17, 1988–1998.
- (47) Mukamel, S. *Chem. Phys.* **1979**, 37, 33–47.